Journal of Nuclear Materials 386–388 (2009) 544–549

Contents lists available at ScienceDirect

Journal of Nuclear Materials

journal homepage: www.elsevier.com/locate/jnucmat

A radiation hardening model of 9%Cr–martensitic steels including dpa and helium

R. Chaouadi [a,b,*], T. Hirai [b], J. Linke [b], G. Pintsuk [b]

[a] SCK•CEN, Mol, Belgium
[b] Forschungszentrum Jülich, EURATOM Association, Jülich, Germany

A B S T R A C T

This paper provides a physically-based engineering model to estimate radiation hardening of 9%Cr-steels under both displacement damage (dpa) and helium. The model is essentially based on the dispersed barrier hardening theory and the dynamic re-solution of helium under displacement cascades but incorporating a number of assumptions and simplifications [Trinkaus, J. Nucl. Mater. 318 (2003) 234–340]. As a result, the kinetics of the damage accumulation kept fixed, its amplitude is fitted on one experimental condition. The model was rationalized on an experimental database that mainly consists of ~9%Cr-steels irradiated in the range of 50–600 °C up to 50 dpa and with a He-content up to 5000 appm. The test temperature effect is taken into account through a normalization procedure based on the change of the Young's modulus and the anelastic deformation that occurs at high temperature. Despite the large experimental scatter, inherent to the variety of the material and irradiation as well as testing conditions, the obtained results are very promising.

1. Introduction

The successful implementation of fusion reactors as an efficient source of electrical power generation requires the solving of a number of critical issues posed by the structural materials. These components are not only submitted to classical loading such as thermo-mechanical stresses but also to neutron irradiation that drastically modifies the mechanical properties. The materials that constitute these components should be therefore qualified to ensure their optimum performance and safe operation. Hence, the interaction of high energy neutrons with metallic structural materials leads to a number of radiation damage phenomena, including hardening, embrittlement, irradiation creep, void swelling, and hydrogen – and helium – embrittlement.

The importance of modeling finds essentially its origin in the possibility to rationalize experimental observations based on physical understanding. By modeling, it is not meant very accurate physical modeling as this is neither feasible nor possible nowadays. Rather, the modeling that is considered here is of engineering nature, with the ultimate goal to incorporate as much as reasonably possible the main parameters needed to describe the phenomenon. In other words, the model should be simplified to its most simple formulation taking into account the major influencing elements and including any physical background whenever available. This means that empirical description or empirical constants are accepted only when no alternative way is available. Such engineering approach of modeling was successfully demonstrated on a number of materials, for example [1,2]. Finally, another important element should be added on the importance of modeling, namely the possibility to act as a quality assurance monitor of the experimental data.

In the following, only the most important ingredients of the model will be given, details can be found elsewhere [3]. Because the model is partially driven by the experimental data, it is important to collect a database on which the model can be calibrated and validated. Therefore, the selection of the experimental databank will be discussed before developing the model and its application to the available data.

2. Experimental database and analysis

In this paper, focus is put on neutron radiation hardening of 9%Cr–ferritic/martensitic steels. The model was developed to allow radiation hardening and embrittlement assessment of these steels. The monitoring of radiation hardening is usually done by examining the yield strength change while radiation embrittlement is monitored by the ductile-to-brittle transition temperature (DBTT). In practice, technological components are designed to operate under loading conditions where the applied/generated stresses are well below the yield strength of the material. Under irradiation, the yield strength of structural materials is changed. In most cases, irradiation results in an increase of the yield strength and therefore the stresses in the component remain in the elastic regime. However, in few cases, in particular at high temperatures, a material softening can also occur. It is essential to verify that this softening cannot induce dimensional instabilities that might affect the operation of the

* Corresponding author. Address: Forschungszentrum Jülich, EURATOM Association, Jülich, Germany.
E-mail address: rachid.chaouadi@sckcen.be (R. Chaouadi).

0022-3115/$ - see front matter © 2009 Elsevier B.V. All rights reserved.
doi:10.1016/j.jnucmat.2008.12.172

component. The DBTT is a reference temperature that is used in structural calculations to provide a lower operating temperature limit of the components. Above this temperature, the material behavior is essentially ductile and therefore any high local stresses can be accommodated by plastic deformation and therefore no unstable fracture would occur. Below the DBTT, unstable brittle fracture is possible jeopardizing the safe operation of the component. In general, the structural materials are chosen such as their operating temperatures are well above the DBTT. Upon irradiation, the DBTT is raised and therefore the lower operation temperature limit is accordingly raised to higher temperatures. Therefore, it is extremely important to capture these effects in order to ensure that the component is operating at any time in the authorized temperature window. However, the DBTT is not an intrinsic material property. It can also be biased in presence of plastic flow localization [4,5]. Another very important material property that is very useful to monitor irradiation effects is the fracture toughness. Irradiation shifts the fracture toughness transition curve to higher temperatures and the ductile crack initiation toughness and the tearing resistance decrease. Unfortunately, the available experimental data are too scarce to be utilized in a modeling perspective. Typically, two materials properties are often reported in literature to monitor irradiation effects, yield strength and DBTT. The yield strength was selected for the irradiation hardening modeling and the resulting irradiation embrittlement is obtained using the load diagram procedure reported elsewhere [3].

Examination of literature data shows that the reported tensile tests are not performed at a single test temperature. Very often, the tensile tests are performed either at room temperature or at the irradiation temperature. There are only few cases where tests were performed in a large temperature range. So, to be consistent when comparing irradiation hardening values obtained at different temperatures, it is necessary to normalize the data to a single reference test temperature, say room temperature. It is known that deformation is a thermally activated process and that the yield strength evolution with test temperature is partially affected through the effect of temperature on the Young's modulus. Within the temperature range that is usually considered, namely, −200 to +600 °C, the slope of the temperature dependence of the Young's modulus is $\alpha \approx 2.67 \cdot 10^{-4}\,\mathrm{K}^{-1}$. However, such a normalization based only on the slope of the Young's modulus is not enough, in particular in the high temperature range. Indeed, it was experimentally found that the Young's modulus variation with test temperature measured with an ultrasonic method exhibits a lower slope than when measured with tensile tests [6], the disagreement increasing with test temperature (see Fig. 1). This can be attributed to the anelastic – time dependent – deformation that introduces a bias when the Young's modulus is determined with a tensile test [7]. So an increase of the temperature dependence slope is required at higher temperatures. If we consider the Hooke relation between stress, strain and Young's modulus, we can write:

$$\sigma_y(T) = E(T) \times \varepsilon_y(T) = (1 - \alpha T) \times E_0 \times (1 - \beta T) \times \varepsilon_{y0}, \quad (1)$$

where σ_y is the stress, ε_y is the strain, E is the Young's modulus and T is the test temperature. The subscript "0" is used as the temperature independent parameters for E, σ_y, and ε_y. The constant α accounts for the linear variation of the Young modulus with temperature and β accounts for the anelastic strain contribution occurring in the high temperature range. Eq. (1) can be approximated by:

$$\sigma_y(T) \approx [1 - \alpha' T] \times E_0 \times \varepsilon_{y0}. \quad (2)$$

The available experimental data support a value of $\alpha' = \alpha + \beta \approx 5.5 \cdot 10^{-4}\,\mathrm{K}^{-1}$ above room temperature [3]. It is important to notice that this is an engineering approximation that was found to agree reasonably well not only with the data shown in Fig. 1 but also with some other independent data [3].

As a result, the normalized room temperature yield strength increase can be written as:

$$\Delta\sigma_y^{RT} \approx \frac{1 - \alpha' T_{RT}}{1 - \alpha' T} \times \Delta\sigma_y^{T}, \quad (3)$$

$$\text{where}: \alpha' = 2.67 \cdot 10^{-4}\,\mathrm{K}^{-1} \quad \text{if } T \le \mathrm{RT},$$
$$\alpha' = 5.5 \cdot 10^{-4}\,\mathrm{K}^{-1} \quad \text{if } \mathrm{RT} < T < 600\,^{\circ}\mathrm{C},$$

where $\Delta\sigma_y^{RT}$ is the yield strength increase at room temperature (RT = 25 °C) and $\Delta\sigma_y^{T}$ is the yield strength increase measured at any other temperature (T). A typical example of application is shown on Fig. 2 where tensile tests performed in the range −150 °C to +300 °C [8] can be normalized to room temperature resulting in a trend curve with a normal experimental uncertainty range of ±25 MPa. All data of the database taken from literature on a variety of 9%Cr-steels were normalized according to the preceding procedure; all details and references of the experimental data are given in [3].

3. Description of the model

The model is based on two components, the first one related to radiation damage (dpa-damage) while the second is related to helium damage [9,10], both associated to the dispersed barrier hardening theory. The parameter that governs the radiation hardening is the number density of the defects, N_d. Therefore, the yield

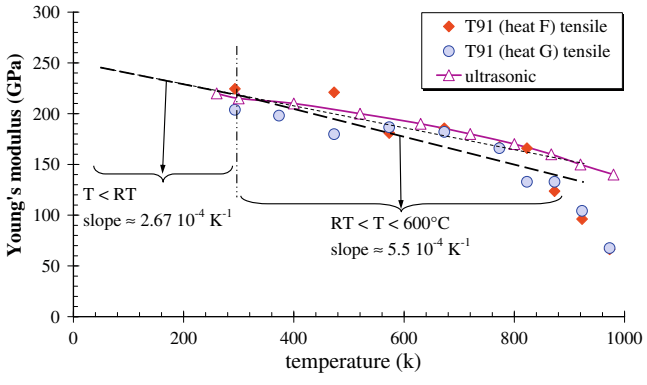

Fig. 1. Young's modulus – test temperature dependence with tensile and ultrasonic method of a 9%Cr-steel, T91 (data from [6]).

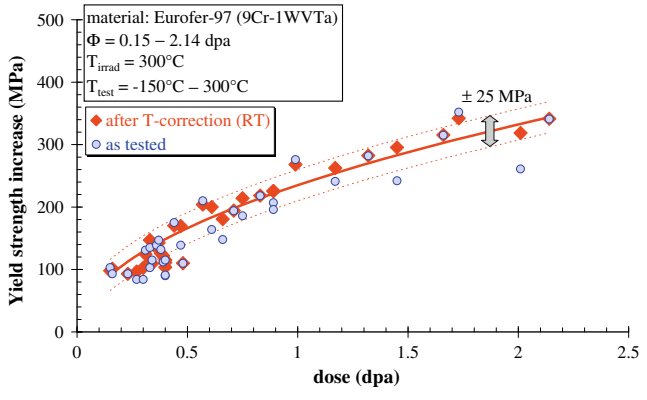

Fig. 2. Effect of the test temperature correction on the yield strength increase of Eurofer-97 irradiated at 300 °C (data from [8]).

strength increase, $\Delta\sigma_y^d$ resulting from the interaction of irradiation defects with a moving dislocation can be approximated by:

$$\Delta\sigma_y^d \approx C_1\sqrt{N_d} \approx C_2\sqrt{\Phi} \approx C\sqrt{1-\exp\left(-\frac{\Phi}{\Phi_0}\right)}, \quad (4)$$

where the C_1, C_2, and C are constants which depend on the material and the irradiation conditions (irradiation temperature), Φ is the neutron fluence and Φ_0 is a constant which was introduced by Whapham and Makin [11] to take defect saturation into account.

To define the kinetics of the temperature dependence of the radiation damage (dpa-component), the annealing (recovery) kinetics is used [12]. Assuming that the recovery mechanism is mainly driven by the escape of vacancies from the zones, an Arrhenius law type of kinetic can be expected [13,14]. Moreover, rather than considering various annealing mechanisms, a single one accounting for the total annealing kinetic is chosen. This means that an 'effective activation energy' rather than several activation energies for the various mechanisms is assumed [3], as illustrated in Fig. 3 where the total annealing curve is obtained from an effective activation energy that accounts for the four mechanisms. Finally, assuming first-order kinetics, the yield strength increase due to displacement damage can be written as:

$$\Delta\sigma_y^{dpa} \approx C_{dpa} \times \exp\left[-v\exp\left(-\frac{\Gamma}{kT_{irrad}}\right)\right] \times \sqrt{1-\exp\left(-\frac{\Phi}{\Phi_0^{dpa}}\right)}, \quad (5)$$

where Γ is the effective activation energy, v is a frequency factor, and k is the Boltzmann constant. The constant C_{dpa} can be fixed on one single experimental condition and should remain constant for all other situations. The model constants Γ and v were experimentally determined using the three following data:

1. specimens irradiated at low temperature (~60 °C) and tested at increasingly higher temperatures (the annealing time corresponds to the holding time at constant temperature before testing) [15–17];
2. specimens implanted with He (constant dpa and He-content) where only the implantation temperature is varied [18,19];
3. specimens irradiated and further annealed [20,21].

It should be noticed that these parameters, Γ and v, are only effective values, including the various annealing mechanisms. Indeed, there are no data where systematic annealing experiments were done to reliably assess each of the mechanisms involved in the recovery process.

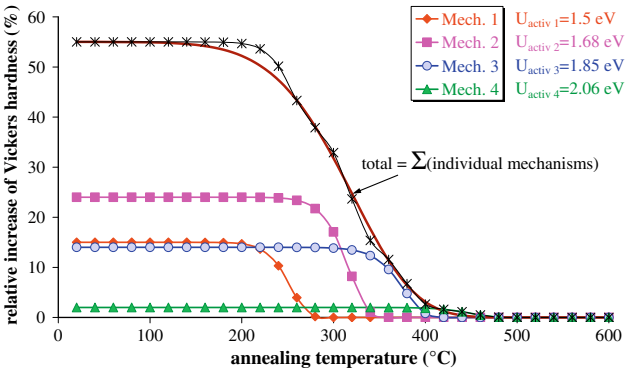

Fig. 3. Illustration of the single effective activation energy obtained from the contribution of four different activations mechanisms [12].

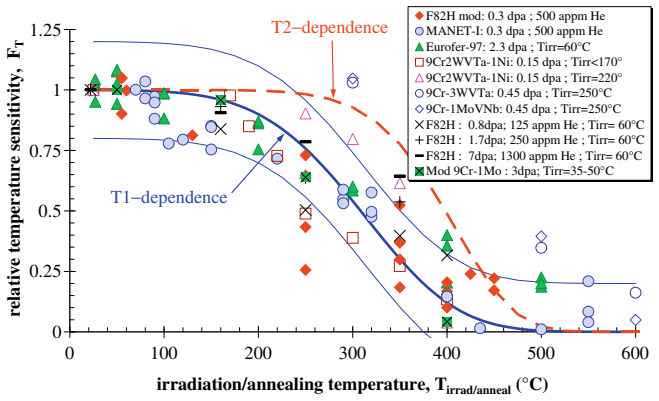

Fig. 4. Irradiation temperature dependence (T1-dependence curve) obtained from experimental data [15–21]. The dashed curve (T2-dependence) is more consistent with the experimental database.

The data are shown on Fig. 4 where the relative temperature sensitivity factor, F_T, is calculated by normalizing the observed relative irradiation hardening with respect either to its initial as-irradiated condition or to the maximum hardening at low temperature. As it can be seen, despite the large scatter, the data can be reasonably well fitted with the adopted model. However, as will be seen later, this fit is not consistent with the database which suggests a dependence according to the dashed curve shown in Fig. 4. This proposed T2-dependence assumes that hardening does not change below 300 °C, in agreement with the experimental data of our database.

To model the hardening induced by He-bubbles, we considered the work of Trinkaus [10] on the kinetics of bubble formation at intermediate temperatures ($0.2 < T/T_m < 0.5$ corresponding roughly to 50–600 °C, T_m being the melting point). Trinkaus gave an analytical description of both the nucleation of bubbles under internal He-generation (primary He-bubbles) and the gas re-solution from existing bubbles (secondary bubbles).

Application of the dispersed barrier hardening model to the He-bubbles leads to the following He-induced yield strength increase component:

$$\Delta\sigma_y^{He} \approx C_{He} \times \{\beta(\dot{\phi} \times (He/dpa))^{m-2}/\dot{\phi}^3 D^2\}^{1/2m}\sqrt{\Phi - \Phi_{He}^{threshold}}, \quad (6)$$

where $\dot{\phi}$ is the dpa-rate, (He/dpa) is the He-to-dpa-rate, $\Phi_{He}^{threshold}$ is the threshold dose below which no He-effect is observed, D is the diffusion coefficient ($D = D_0\exp\left(-\frac{U_a}{kT_{irrad}}\right)$, $U_a = 0.93$ eV is the He-migration energy, $D_0 \approx 10^{-5}$ m^2 s^{-1} is a temperature independent constant) and β and m are constants. As for the dpa-component, the amplitude, characterized by the constant C_{He} is experimentally fitted on one single condition and kept constant for all other experimental conditions. Finally, the total contribution of both dpa and He to hardening can be obtained by a linear or a quadratic addition of the two components. The choice of the appropriate superposition law will be based on the best agreement to the experimental data. Of course, different combinations of the amplitude of the two components are required to make such an assessment.

Eqs. (5) and (6) allow determining the total yield strength increase as a function of a limited number of variables, namely, the irradiation temperature, dpa-rate, the total dpa and the He-to-dpa-rate or He-rate. All other parameters (v, Γ, Φ_0, D_0, U_a, m, C_{dpa}, C_{He}, β, $\Phi_{He}^{threshold}$) are constants, and will be given later for the appropriate superposition law and temperature dependence that will be selected. Application of this model is presented in the next section.

4. Results and discussion

First, it is important to mention that are the yield strength data considered in the database were evaluated according to Eq. (3) to remove the test temperature dependence. The yield strength increase as a function of the displacement damage ($\Delta\sigma_y$-dpa) taken from the database where He-content is below 1000 appm (0.1%) indicate that despite the large scatter, there is no significant effect of temperature in the range 50–325 °C. Note that the experimental data used in the database [4,15,22–52] are different from those used for deriving Fig. 4 [15–21]. A significant hardening decrease is noticed at 365 °C and higher. Above about 430 °C, no hardening occurs and even some softening occurs. The effect of irradiation temperature is clearly not consistent with the data shown in Fig. 4. The reasons of this disagreement are at this stage unknown. Details on the testing conditions are necessary to identify the possible reasons. Nevertheless, if the negligible effect of irradiation temperature in the range 50–325 °C is taken into account, the temperature sensitivity factor should be modified according to the dashed curve shown on Fig. 4. It should also be noticed that the experimental data where the yield strength after irradiation has decreased rather than increased cannot be correctly modeled. Irradiation softening, which occurs in the high temperature range (450–600 °C), was indeed not incorporated in the model. So the temperature sensitivity remains an open issue and it will be necessary to correctly take this key parameter into account before being able to model irradiation effects.

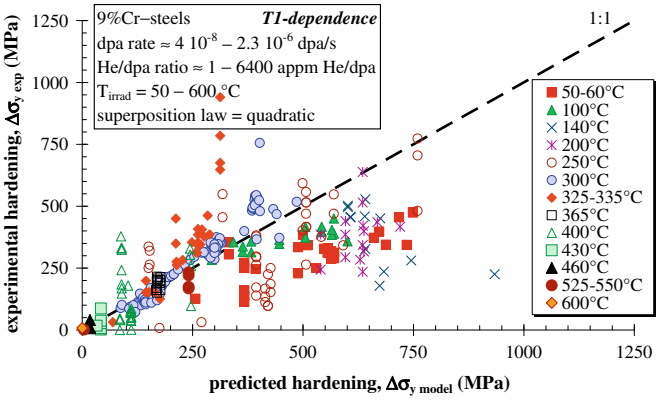

Fig. 5. Comparison between experimental data [4,15,22–52] and model prediction considering the irradiation temperature sensitivity dependence of the full curve (T1-dependence) shown in Fig. 4.

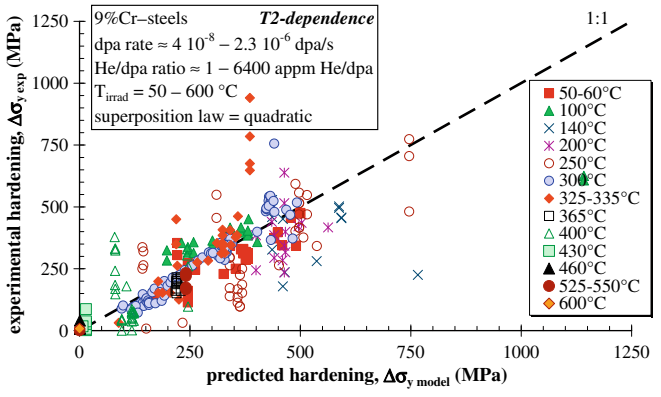

Fig. 6. Comparison between experimental data [4,15,22–52] and model prediction considering the irradiation temperature sensitivity dependence of the dashed curve (T2-dependence) shown in Fig. 4.

Examination of the database shows that the effect of helium is not obvious below about 500 appm He. Therefore, the threshold value of 500 appm He below which the He-contribution to hardening is neglected was fixed [3].

Assuming a quadratic superposition law, application of the model to the database is shown in Figs. 5 and 6, for the two temperature (T1- and T2-dependence) sensitivity trends shown in Fig. 4. These two Figures compare the experimentally measured yield strength increase to the predicted one using Eqs. (5) and (6) assuming a quadratic superposition. At high dpa and high He-content, the predicted hardening is significantly overestimating the experimental one. This was expected from the He-contribution to hardening that does not saturate. Unfortunately, the available data do not allow yet the determination of the saturation value. If the linear superposition law is adopted, the whole picture does not significantly change; the scatter is too high to clearly distinguish possible changes.

Most of the data shown in Figs. 5 and 6 are neutron-irradiated data and therefore with little He-generation. It is interesting to examine the validity of the model for specimens with significant He-content, or He/dpa-rate. Figs. 7 and 8 show two examples where the He/dpa-ratio is around 6400 appm He/dpa implanted at 325 and 550 °C, respectively. Unfortunately, for all these data, the dpa-level does not exceed ~1 dpa. Nevertheless, the agreement between experimental data and model prediction is reasonable in the investigated temperature range (150–550 °C). Note that because of the high dpa-rates used during He-implantation (<100 h), softening is not expected to occur and this is supported by the data shown on Fig. 8.

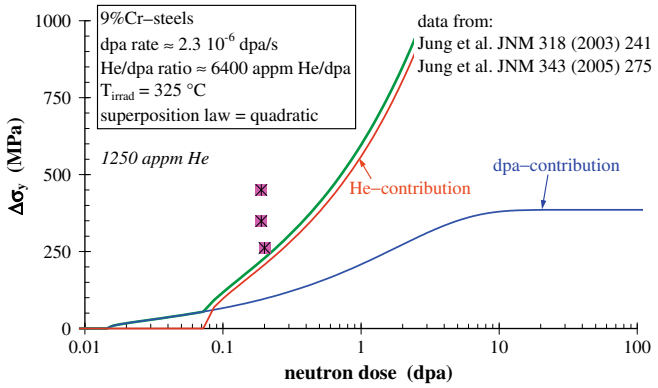

Fig. 7. Comparison between experimental data and model prediction of high He-content specimens implanted at 325 °C.

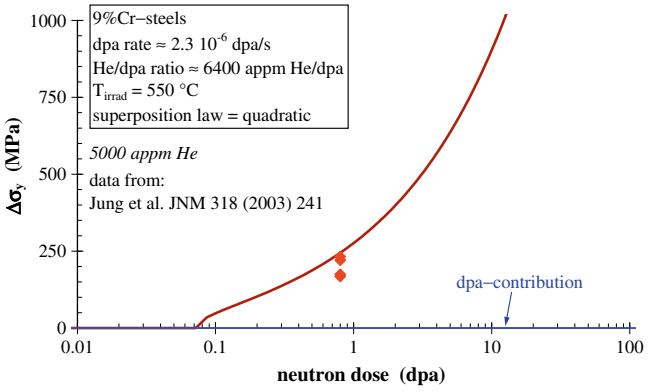

Fig. 8. Comparison between experimental data and model prediction of high He-content specimens implanted at 550 °C.

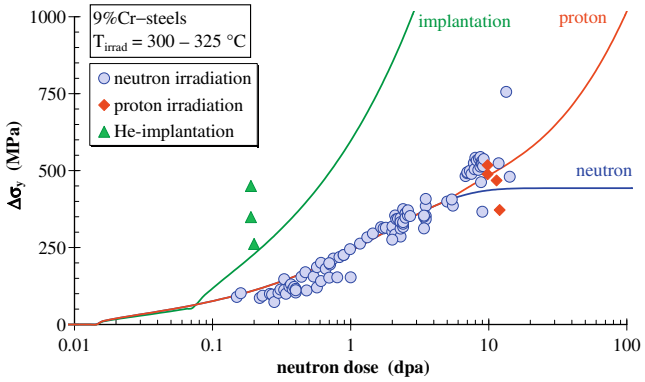

Fig. 9. Application of the model and comparison to the experimental data at ~300 °C.

If a quadratic superposition law is selected together with the T2-temperature dependence, the following parameters of the model should be used: C_{dpa} = 500 MPa, Γ = 0.9 eV, $\nu = 10^7$, Φ_0^{dpa} = 3 dpa, C_{He} = 330 MPa, $D_0 = 10^{-5}$ m^2 s^{-1}, U_a = 0.93 eV, $\beta \approx 10^{-30}$ m^4, $\Phi_{He}^{threshold} = \Phi_{500\ appm\ He}$ (dose corresponding to 500 appm He), and m = 7 [3]. This set of constants is kept identical for all conditions, the variables are only the irradiation temperature (T_{irrad}), the dpa-rate ($\dot{\phi}$) and the He/dpa-ratio (He/dpa). An illustration of the application of the model is given in Fig. 9 for neutron and proton irradiation as well as He-implantation at around 300 °C.

Globally, the agreement between experimental and predicted hardening is reasonable if all uncertainties and adopted assumptions are taken into consideration. It should be emphasized that from an engineering point of view, a mean curve is not a must but lower/upper bounds would offer a frame for designers that they can evaluate their safety margins.

5. Conclusions

This work has shown the possibility of providing an engineering tool to evaluate irradiation effects including both dpa and helium damage of 9%Cr–ferritic/martensitic steels. It is clear that the performance of such an engineering modeling will depend much on the input data, namely the experimental data on which a number of parameters were based. Of course, all underlying mechanisms are not taken into account in order to limit the number of variables. Instead, only two major components were considered, dpa-damage on one hand and He-damage on the other hand.

One of the main difficulties encountered in this work is the reliability of the experimental data. This was illustrated by the major conflict observed on the effect of irradiation temperature. Other difficulties are related to the large number of variables considered in the database. Actually there are no or negligibly few experiments with a single – isolated variable. Materials are not all similar from both chemical composition and heat treatments, the irradiation conditions (reactor type, neutron spectrum) are not the same and testing conditions are not similar as well. So, it is not surprising that some inconsistencies can be observed and therefore the model capabilities should be taken with large uncertainties. A number of data are also missing, for instance both high dpa high He-content data are desirable. It is clear that an urgent call for a reliable database becomes obvious to improve modeling performances. Such experimental data combined with modeling efforts will lead to a reliable assessment of irradiation effects on 9%Cr-steels.

Acknowledgements

This work was performed within the HELENA project, in the frame of an Intra European Fellowship sponsored by the European Commission. The views and opinions expressed herein do not necessarily reflect those of the European Commission. Grateful acknowledgements go to Professor H. Ullmaier, Dr H. Trinkaus, and Dr P. Jung for their encouragements and fruitful discussions.

References

[1] E.D. Eason, J.E. Wright, G.R. Odette, Improved embrittlement correlations for reactor pressure vessel steels, NUREG/CR-6551, November, 1998.
[2] T. Yamamoto, G.R. Odette, H. Kishimoto, J.W. Rensman, P. Miao, J. Nucl. Mater. 356 (2006) 27.
[3] R. Chaouadi, Neutron-irradiation+helium hardening and embrittlement modeling of 9%Cr-steels in an engineering perspective – HELENA, Schriften des Forschungszentrums Jülich, Reihe Energie & Umwelt, vol. 20, 2008.
[4] R. Chaouadi, J. Nucl. Mater. 360 (2007) 75.
[5] R. Chaouadi, J. Nucl. Mater. 372 (2008) 379.
[6] K. Sawada, T. Ohba, H. Kushima, K. Kimura, Mater. Sci. Eng. A 394 (2005) 36.
[7] J.R. Davis, Tensile Testing, 2nd Ed., ASM International, 2004.
[8] E. Lucon, Mechanical properties of the European reference RAFM steel (Eurofer-97) before and after irradiation at 300 °C (0.3–2 dpa), SCK•CEN Report BLG-962, 2003.
[9] H. Ullmaier, Nucl. Fus. 24 (1984) 1039.
[10] H. Trinkaus, J. Nucl. Mater. 318 (2003) 234.
[11] A.D. Whapham, M.J. Makin, Philos. Mag. 5 (1960) 237.
[12] D. Pachur, Nucl. Technol. 59 (1982) 463.
[13] C.C. Dollins, Radiat. Eff. 16 (1972) 271.
[14] D.J. Harvey, M.S. Wechsler, Kinetics of annealing of irradiated surveillance pressure vessel steels, in: H.R. Brager, J.S. Perrin (Eds.), Effects of Radiation on Materials, ASTM STP 782, ASTM, Philadelphia, 1982, p. 505.
[15] J. Rensman, NRG irradiation testing: Report on 300 °C and 60 °C irradiated RAFM steels, NRG Report NRG20023/05.68497/P, 2005.
[16] Y. Dai, X. Jia, S.A. Maloy, J. Nucl. Mater. 343 (2005) 241.
[17] S.A. Maloy, M.R. James, G. Willcutt, W.F. Sommer, M. Sokolov, L.L. Snead, M.L. Hamilton, F. Garner, J. Nucl. Mater. 296 (2001) 119.
[18] R. Lindau, A. Möslang, D. Preininger, M. Rieth, H.D. Röhrig, J. Nucl. Mater. 271&272 (1999) 450.
[19] E. Daum, K. Ehrlich, M. Schirra (Eds.), Development of ferritic/martensitic steels for fusion technology, FZKA-5848, 1997.
[20] F. Abe, T. Noda, H. Araki, M. Narui, H. Kayano, J. Nucl. Mater. 191–194 (1992) 845.
[21] R. Kasada, A. Kimura, H. Matsui, M. Narui, J. Nucl. Mater. 258–263 (1998) 1199.
[22] A. Alamo, J.L. Bertin, V.K. Shamardin, P. Wident, J. Nucl. Mater. 367–370 (2007) 54.
[23] N. Baluc, R. Schäublin, C. Bailat, F. Paschoud, M. Victoria, J. Nucl. Mater. 283–287 (2000) 731.
[24] J.C. Brachet, X. Averty, P. Lamagnère, A. Alamo, F. Rozenblum, O. Raquet, J.L. Bertin, Behavior of different austenitic stainless steels, conventional, reduced activation (RA) and ODS chromium-rich ferritic–martensitic steels under neutron irradiation in PWR environments, in: T. Rosinski, M.L. Grossbeck, T.R. Allen, A.S. Kumar (Eds.), Effects of Radiation on Materials, ASTM STP 1405, ASTM, West Conshohocken, 2001, p. 500.
[25] T.S. Byun, K. Farrell, E.H. Lee, L.K. Mansur, S.A. Maloy, M.R. James, W.R. Johnson, J. Nucl. Mater. 303 (2002) 34.
[26] Y. Dai, X.J. Jia, K. Farrell, J. Nucl. Mater. 318 (2003) 192.
[27] Y. de Carlan, X. Averty, J.C. Brachet, J.L. Bertin, F. Rozenblum, O. Rabouille, A. Bougault, J. ASTM Int. 2 (8) (2005).
[28] K. Farrell, T.S. Byun, J. Nucl. Mater. 296 (2001) 129.
[29] J. Henry, X. Averty, Y. Dai, P. Lamagnère, J.P. Pizzanelli, J.J. Espinas, P. Wident, J. Nucl. Mater. 318 (2003) 215.
[30] P. Jung, J. Henry, J. Chen, J.C. Brachet, J. Nucl. Mater. 318 (2003) 241.
[31] P. Jung, J. Henry, J. Chen, J. Nucl. Mater. 343 (2005) 275.
[32] P. Jung, J. Chen, H. Klein, J. Nucl. Mater. 356 (2006) 88.
[33] R.L. Klueh, D.J. Alexander, Tensile and Charpy impact properties of irradiated reduced-activation ferritic steels, in: R.K. Nanstad, M.L. Hamilton, F.A. Garner, A.S. Kumar (Eds.), Effects of Radiation on Materials, ASTM STP 1325, ASTM, 1999, p. 911.
[34] R.L. Klueh, J.M. Vitek, J. Nucl. Mater. 150 (1987) 272.
[35] R.L. Klueh, J.M. Vitek, J. Nucl. Mater. 161 (1989) 13.
[36] R.L. Klueh, J. Nucl. Mater. 179–181 (1991) 728.
[37] R.L. Klueh, D.J. Alexander, J. Nucl. Mater. 186 (1994) 736.
[38] R.L. Klueh, P.J. Maziasz, J. Nucl. Mater. 187 (1992) 43.
[39] R.L. Klueh, J.J. Kai, D.J. Alexander, J. Nucl. Mater. 225 (1995) 175.
[40] R.L. Klueh, D.J. Alexander, J. Nucl. Mater. 233–237 (1996) 336.
[41] R.L. Klueh, D.J. Alexander, M. Rieth, J. Nucl. Mater. 273 (1999) 146.
[42] R.L. Klueh, M.A. Sokolov, K. Shiba, Y. Miwa, J.P. Robertson, J. Nucl. Mater. 283–287 (2000) 478.
[43] R.L. Klueh, N. Hashimoto, M.A. Sokolov, K. Shiba, S. Jitsukawa, J. Nucl. Mater. 357 (2006) 156.
[44] H. Kurishita, H. Kayano, M. Narui, A. Kimura, M.L. Hamilton, D.S. Gelles, J. Nucl. Mater. 212–215 (1994) 730.
[45] E. Lucon, A. Almazouzi, Mechanical response to irradiation, SCK•CEN Report BLG-986, 2004.
[46] M.H. Mathon, Y. de Carlan, X. Averty, A. Alamo, C.H. de Novion, J. ASTM Int. 2 (9) (2005).

[47] J.L. Séran, V. Lévy, P. Dubuisson, D. Gilbon, A. Maillard, A. Fissilo, H. Touron, R. Cauvin, A. Chalony, E. Le Boulbin, Behavior under neutron irradiation of the 15-15Ti and EM10 steels used as standard materials of the Phénix fuel subassembly, in: R.E. Stoller, A.S. Kumar, D.S. Gelles (Eds.), Effects of Radiation on Materials, ASTM STP 1125, ASTM, Philadelphia, 1992, p. 1209.
[48] J.L. Séran, A. Alamo, A. Maillard, H. Touron, J.C. Brachet, P. Dubuisson, O. Rabouille, J. Nucl. Mater. 212–215 (1994) 588.
[49] V.K. Shamardin, V.N. Golovanov, T.M. Bulanova, A.V. Povstyanko, A.E. Fedoseev, Z.E. Ostrovsky, Y.D. Goncharenko, J. Nucl. Mater. 307–311 (2002) 229.
[50] E. Wakai, T. Taguchi, T. Yamamoto, F. Takada, J. Nucl. Mater. 329–333 (2004) 1133.
[51] E. Wakai, S. Jitsukawa, H. Tomita, K. Furuya, M. Sato, K. Oka, T. Tanaka, F. Takada, T. Yamamoto, Y. Kato, Y. Tayama, K. Shiba, S. Ohnuki, J. Nucl. Mater. 343 (2005) 285.
[52] Wakai, M. Ando, T. Sawai, K. Kikuchi, K. Furuya, M. Sato, K. Oka, S. Ohnuki, H. Tomita, T. Tomita, Y. Kato, F. Takada, J. Nucl. Mater. 356 (2006) 95.